ASBMB MOLECULAR & CELLULAR PROTEOMICS MCP

Comparative Proteomics Analysis of Differentially Expressed Proteins in Chickpea Extracellular Matrix during Dehydration Stress*[S]

Deepti Bhushan, Aarti Pandey, Mani Kant Choudhary, Asis Datta, Subhra Chakraborty‡, and Niranjan Chakraborty§

Water deficit or dehydration is the most crucial environmental factor that limits crop productivity and influences geographical distribution of many crop plants. It is suggested that dehydration-responsive changes in expression of proteins may lead to cellular adaptation against water deficit conditions. Most of the earlier understanding of dehydration-responsive cellular adaptation has evolved from transcriptome analyses. By contrast, comparative analysis of dehydration-responsive proteins, particularly proteins in the subcellular fraction, is limiting. In plants, cell wall or extracellular matrix (ECM) serves as the repository for most of the components of the cell signaling process and acts as a frontline defense. Thus, we have initiated a proteomics approach to identify dehydration-responsive ECM proteins in a food legume, chickpea. Several commercial chickpea varieties were screened for the status of dehydration tolerance using different physiological and biochemical indexes. Dehydration-responsive temporal changes of ECM proteins in JG-62, a relatively tolerant variety, revealed 186 proteins with variance at a 95% significance level statistically. The comparative proteomics analysis led to the identification of 134 differentially expressed proteins that include predicted and novel dehydration-responsive proteins. This study, for the first time, demonstrates that over a hundred ECM proteins, presumably involved in a variety of cellular functions, *viz.* cell wall modification, signal transduction, metabolism, and cell defense and rescue, impinge on the molecular mechanism of dehydration tolerance in plants. *Molecular & Cellular Proteomics 6:1868–1884, 2007.*

Environmental stress is a primary cause of crop loss worldwide, resulting in average yield losses of more than 50% for major crops every year (1, 2). Among the unfavorable environmental conditions, water deficit or dehydration is the most significant factor that adversely affects plant growth, development, and productivity. In recent years, the physiological and molecular basis for plant responses to dehydration tolerance has been the subject of intense research (3, 4). It is now well established that plants, being sessile, have evolved many adaptations to counteract dehydration. These adaptations are classified into four categories: dehydration avoidance (developmental and physiological traits), dehydration tolerance (physiological and biochemical adaptations), dehydration escape, and dehydration recovery (5). Dehydration response in plants is a complex phenomenon, and the exact structural and functional modification caused by dehydration is poorly understood. Thus, understanding the responses of plants to dehydration is of importance not only for basic research but also an attractive target for improving such stress tolerance. A few characteristics such as osmotic adjustment (OA)[1] and cell membrane stability are recognized as effective components of dehydration tolerance in many crops. These are expressed in terms of relative water content (RWC) of the plant, accumulation of compatible solutes like proline, and increased permeability of ions and electrolytes. In addition the status of photosynthetic machinery has been considered as an ideal index to monitor the health and vitality of plants during dehydration (6).

Most studies on dehydration to date have mainly focused on the changes in gene expression, whereas there is far less information available on their functional products. The changes in gene expression are regulated by a number of different, and potentially overlapping, signal transduction pathways (7, 8). Nevertheless the significance of these genes in dehydration tolerance is incomplete without the knowledge of their function. Hence proteomics analysis is necessary to reveal the plasticity of gene expression because this allows the global analyses of gene products and physiological state

From the National Centre for Plant Genome Research, Aruna Asaf Ali Marg, New Delhi 110067, India

Received, January 18, 2007, and in revised form, August 1, 2007
Published, MCP Papers in Press, August 7, 2007, DOI 10.1074/mcp.M700015-MCP200

[1] The abbreviations used are: OA, osmotic adjustment; DRP, dehydration-responsive protein; ECM, extracellular matrix; 2-DE, two-dimensional electrophoresis; ROS, reactive oxygen species; RWC, relative water content; MDA, malondialdehyde; SOTA, self-organizing tree algorithm; WP, water potential; WAK, wall-associated kinase; NDK, nucleotide-diphosphate kinase; CHRK, chitinase-specific receptor kinase; GRP, glycine-rich protein.

of cells. However, the application of a proteomics approach at the whole cell level is limited by several factors such as protein abundance, size, hydrophobicity, and other electrophoretic properties (9). The compartment-specific proteome is thus recommended because fractionated subsets of proteins provide the suitable information in which they exert their particular function (10–12). Plant cell wall or extracellular matrix (ECM) is the first compartment that senses the stress signals, transmits them to the cell interior, and eventually influences the cell fate decision (11, 13). Increasing evidence suggests that there is continuous cross-talk between ECM and the cytoskeleton network (14). Within the past few years, there have been rapid advances in ECM research (15). However, most research interest on ECM has been in the carbohydrate components due to their structural role and commercial interests, whereas the study of the complexity of ECM proteins remained secondary (16).

Legumes are valuable agricultural and commercial crops mostly cultivated in the arid and semiarid part of the world and are particularly important as nutrient sources for the human diet and animal feed (17). They are among the few self-autonomous organisms capable of fixing carbon and nitrogen, and the estimates of nitrogen fixation by food legumes is about 300 kg/hectare/year. Chickpea is the most important food legume and ranks third in terms of total global production (18, 19). The susceptibility of chickpea to dehydration severely reduces the yield, and its productivity has remained historically low. Although the simultaneous changes in gene expression and physiological responses strongly suggest that induced proteins play a role in these responses, the correlation between their expression and the level of stress tolerance in different genotypes has rarely been studied. In this study, dehydration-induced physiological responses were monitored in eight commercial chickpea varieties using various parameters, *viz.* RWC, proline accumulation, lipid peroxidation, electrolyte leakage, and the status of photosynthetic pigments. The altered physiological status of the cell in response to dehydration was correlated with temporal changes in the ECM/cell wall proteome in a tolerant variety, JG-62. In a previous study, we reported the ECM proteome map of chickpea (11). Here we used the ECM-specific comparative proteome of chickpea to identify novel components involved in dehydration tolerance with a wider aim to use them in a future crop improvement program. The quantitative image analysis revealed 163 protein spots that changed their intensities significantly ($p < 0.05$) by more than 2.5-fold at least at one time point during dehydration. A total of 134 differentially expressed ECM proteins were identified during the course of dehydration using classical two-dimensional electrophoresis (2-DE) coupled with LC-MS/MS. The comparison of the dehydration-responsive ECM proteome in chickpea revealed predicted and unexpected components indicating their possible role in dehydration tolerance.

EXPERIMENTAL PROCEDURES

Plant Growth, Maintenance, and Dehydration Treatment—Seeds of eight commercial chickpea (*Cicer arietinum* L.) cultivars (Vijay, WR-315, Annigiri, CPS-1, K-850, JG-62, C-235, and ICCV2) were obtained from the International Crops Research Institute for the Semi-Arid Tropics, Hyderabad, India and grown in a mixture of soil and soilrite (2:1, w/w; 10 plants/1.5-liter-capacity pot with 18-cm diameter) in an environmentally controlled growth room. The seedlings were maintained at 25 ± 2 °C, 50 ± 5% relative humidity under a 16-h photoperiod (270 μmol m^{-2} s^{-1} light intensity). The pots were provided with 100 ml of water every day that maintained the soil moisture content to approximately 30%. A gradual dehydration condition was applied on the 3-week-old seedlings for a period of 7 days by withdrawing water, and tissues were harvested at every 24 h. The pots were then rewatered allowing complete recovery of the stressed seedlings for 24 h. The unstressed and the stressed plants were kept in parallel in the same growth room. The samples from the unstressed (control) plants were collected every day during the course of the dehydration experiment and were finally pooled. The tissues were harvested, instantly frozen in liquid nitrogen, and stored at −80 °C unless described otherwise.

Determination of Relative Water Content—Chickpea tissues were collected and immediately weighed (fresh weight (FW)). The tissues were rehydrated in water for 24 h until fully turgid, surface-dried, reweighed (turgid weight (TW)) followed by oven drying at 80 °C for 48 h, and reweighed (dry weight (DW)). The RWC was calculated by the following formula: RWC (%) = (FW − DW/TW − DW) × 100 (20). The experiment was carried out in triplicates.

Proline Estimation—Free proline content was measured as described earlier (21). The tissues were homogenized in 3% aqueous sulfosalicylic acid, and the homogenate was centrifuged at 9000 × *g*. The reaction mixture consisted of 2 ml of supernatant, 2 ml of acid ninhydrin, and 2 ml of glacial acetic acid, which was boiled at 100 °C for 1 h. After termination of the reaction on ice, the reaction mixture was extracted with 4 ml of toluene, and the absorbance was read at 520 nm. The assays were done in triplicates using corrected weight calculated for the actual moisture content of tissue at each time point. Proline was calculated according to the following formula: proline (mg/g) = 36.6 × A_{520} × volume/2 × fresh weight.

Pigment Estimation—Tissues harvested at different time points were ground in 80% chilled acetone. The supernatant was taken for determination of photosynthetic pigments: chlorophyll *a* (mg/g) = ((12.7 × A_{663} − 2.69 × A_{645}) v/w), chlorophyll *b* (mg/g) = ((22.9 × A_{645} − 4.68 × A_{663}) v/w), and carotenoid (mg/g) = (((1000 × A_{470}) − (3.27 × chlorophyll *a* + 1.04 × chlorophyll *b*))/227 v/w). The experiments were done in triplicates using corrected tissue weights calculated for actual moisture content of the tissue at the respective time points (22).

Determination of Lipid Peroxidation—Lipid peroxidation was estimated in terms of malondialdehyde (MDA) production. Fresh chickpea tissues were ground in 5% TCA. One part of the supernatant was mixed with four parts of 0.5% thiobarbituric acid prepared in 20% TCA and heated at 95 °C for 30 min. Absorbance at 532 nm was measured and corrected for nonspecific absorbance at 600 nm. The pellet was washed in 100% chilled acetone and suspended in 0.1 N NaOH to estimate total protein using Bradford reagent. Oxidized MDA was calculated according to the following formula: MDA (μg/mg) = ((A_{532} − A_{600}) × volume × 100)/(155 × total protein (mg)). The experiments were carried out in triplicates using corrected weights calculated for actual moisture content of the seedlings at each time point (22).

Electrolyte Leakage Assay—Electrolyte leakage was assayed by estimating the ions leaching from the leaflets into Milli-Q water. Plant materials were placed in 20 ml of Milli-Q in two sets. The first set was

kept at room temperature for 4 h, and its conductivity (C1) was recorded using a conductivity meter. The second set was autoclaved, its conductivity was also recorded (C2), and electrolyte leakage ($1 - (C1/C2)) \times 100$ was calculated. The experiments were carried out in triplicates.

Isolation of ECM Fraction and 2-DE—The ECM protein fraction was essentially isolated as described earlier (11). In brief, the tissues were ground to powder in liquid nitrogen with 0.3% (w/w) polyvinylpolypyrrolidone and transferred to an open mouthed 50-ml centrifuge tube. Immediately tissue powder was homogenized in homogenizing buffer (5 mM K_3PO_4, pH 6.0, 5 mM DTT, 1 mM PMSF) for 1–2 min. The cell wall fraction was recovered by differential centrifugation at 1000 $\times$ *g* for 5 min at 4 °C. The pellet thus obtained was washed 10 times with excess deionized water. The purified ECM fraction was suspended in 3 volumes (w/v) of extraction buffer (200 mM $CaCl_2$, 5 mM DTT, 1 mM PMSF, 0.3% (w/w) polyvinylpolypyrrolidone) and extracted on a shaking platform for 45 min at 4 °C. Proteins were separated from the insoluble ECM fraction by centrifugation (10,000 $\times$ *g*) for 10 min at 4 °C and filtered through a 0.45-μm filter. The filtrate was concentrated using Centricon YM3 and then dialyzed overnight against 1000 volumes of deionized water with one change. The concentration of the protein extract was determined by Bradford assay (Bio-Rad).

Isoelectric focusing was carried out with 125 μg of protein sample in 250 μl of two-dimensional rehydration buffer for 13-cm gel strips. Protein was loaded by the in-gel rehydration method onto IEF strips (pH range, 4–7). Electrofocusing was performed using an IPGphor system (Amersham Biosciences) at 20 °C for 30,000 V-h. The focused strips were subjected to reduction with 1% (w/v) DTT in 10 ml of equilibration buffer (6 M urea, 50 mM Tris-HCl (pH 8.8), 30% (v/v) glycerol and 2% (w/v) SDS) followed by alkylation with 2.5% (w/v) iodoacetamide in the same buffer. The strips were then loaded on top of 12.5% polyacrylamide gels for SDS-PAGE. The electrophoresed proteins were stained with a Silver Stain Plus kit (Bio-Rad).

Image Acquisition and Data Analysis—Gel images were digitized with a Bio-Rad FluorS system equipped with a 12-bit camera. PDQuest version 7.2.0 (Bio-Rad) was used to assemble a first level match set (master image) from three replicate 2-DE gels. Experimental molecular mass and pI were calculated from digitized 2-DE images using standard molecular mass marker proteins. Each spot included on the standard gel met several criteria: it was present in at least two of the three gels and was qualitatively consistent in size and shape in the replicate gels. We defined "low quality" spots as those with a quality score less than 30; these spots were eliminated from further analysis. The remaining high quality spot quantities were used to calculate the mean value for a given spot, and this value was used as the spot quantity on the standard gel. The first level match set spot densities were normalized against the total density in the gel image. The replicate gels used for making the first level match set had at least a correlation coefficient value of 0.8. After obtaining the first level match sets, a second level match set that allowed a comparison of the standard gels from each of the time points was obtained. A second normalization was done with a set of three unaltered spots identified from across the time points. From this match set, the filtered spot quantities from the standard gels were assembled into a data matrix of high quality spots from the eight time points for further analysis.

Protein Identification and Expression Clustering—Protein samples were destained and trypsin-digested, and peptides were extracted according to standard techniques (23). Peptides were analyzed by electrospray ionization time-of-flight mass spectrometry (LC/MS/TOF) using an Agilent 1100 Series HPLC system (Agilent Technologies) coupled to a Q-STAR Pulsar *i*mass spectrometer (Applied Biosystems). Tryptic peptides were loaded onto a Zorbax® SB-C_{18} column (15-cm length; Agilent Technologies) and separated with a linear gradient of water, acetonitrile, 0.1% formic acid (v/v). The MS/MS data were extracted using Analyst Software version 1.4.1 (Applied Biosystems). Peptides were identified by searching the peak list against the Mass Spectrometry Protein Sequence Database (MSDB) September 29, 2005 (2,344,227 sequences; 779,380,795 residues) using the Mascot version 2.1 (Matrix Science) search engine. Because the chickpea genome sequence is not known, a homology-based search was performed. The database search parameters were taxonomy, Viridiplantae (green plants; 195,697 sequences); peptide tolerance, $\pm$1.2 Da; fragment mass tolerance, $\pm$0.6 Da; maximum allowed missed cleavage, 1; instrument type, ESI-Q-TOF. Protein scores were derived from ion scores as a nonprobabilistic basis for ranking protein hits and protein scores as the sum of a series of peptide scores. The score threshold to achieve $p < 0.05$ is set by the Mascot algorithm and is based on the size of the database used in the search. The details regarding the precursor ion mass, expected molecular weight, theoretical molecular weight, delta, score, rank, charge, number of missed cleavages, *p* value, and the peptide sequence for proteins identified with a single peptide are listed in Supplemental Document 1. In addition the fragment spectra for these proteins are provided in Supplemental Document 2. Wherein there were more than one accession number for the same peptide, the match was considered in terms of putative function. In the case of the same protein being identified in multiple spots where several peptides were found to be shared by the isoforms, a differential expression pattern was observed for each of the candidates, and thus the proteins were listed as independent entities. The function of each of the identified protein was analyzed in view of the metabolic role of the candidate protein in the extracellular matrix. Because the functional annotation is based on Pfam and InterPro, the functional redundancy, if any, is thus greatly minimized.

SOTA (self-organizing tree algorithm) clustering was performed on the log-transformed -fold induction expression values across eight time points by using MultiExperiment Viewer (MEV) software (The Institute for Genomic Research). The clustering was done with the Pearson correlation as distance with 10 cycles and a maximum cell diversity of 0.8 (24).

RESULTS AND DISCUSSION

Screening of Chickpea Varieties for Dehydration Tolerance—Dehydration tolerance, in plants, is attained by two major physiological events: (*a*) the maintenance of a high water status during stress and (*b*) the maintenance of function at low water status. RWC is considered to be the best integrated measure of plant water status, which represents variations in water potential (WP), turgor potential, and OA. The advantage of RWC over WP for assessing genetic differences in dehydration resistance is that although having the same WP genotypes may vary in their RWC due to the respective difference in OA. The choice of RWC as the best representation of plant water status in terms of genetic variation is also supported by genetic association between RWC and plant production under dehydration (25). In this study, eight commercial varieties of chickpea were evaluated for their relative tolerance to dehydration. The initial soil moisture content was ~30%; this gradually decreased to zero after 72 h of withdrawal of water. Upon applying dehydration stress, the seedlings of all the varieties showed a steady increase in RWC around 72 h after a gradual decline at initial stages. This could be substantiated by the observation that proline content increased during 24–72 h causing probable OA. When com-

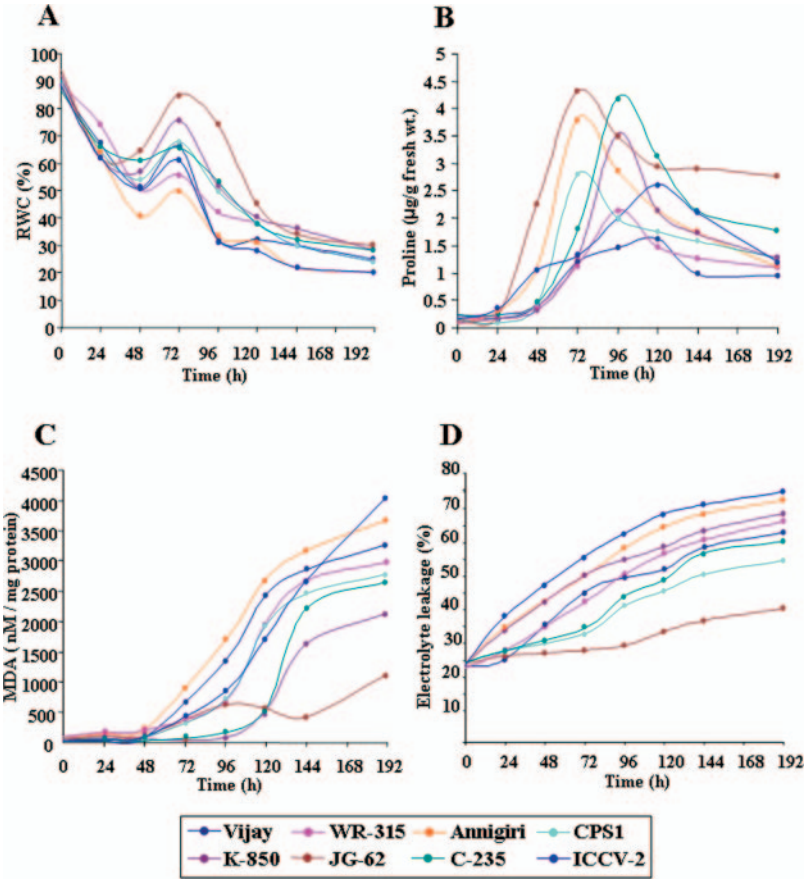

FIG. 1. **Effect of dehydration on water status, proline accumulation, and cell membrane stability.** Comparative analysis of RWC (*A*), proline accumulation (*B*), MDA (*C*), and electrolyte leakage (*D*) between eight varieties of chickpea in a time-dependent manner under dehydration. All experiments were done in triplicates ($n = 3$), and average mean values were plotted against duration of dehydration.

pared with the other varieties, maximum proline accumulation was observed in JG-62 during dehydration; this can be attributed to the maximum (85%) increase in RWC (Fig. 1, *A* and *B*).

The capacity to avoid or repair membrane damage during dehydration processes is pivotal for the maintenance of membrane integrity, especially for those membranes in which functional proteins are embedded. To determine the level of membrane integrity, the status of electrolyte leakage was monitored in all eight varieties under dehydration. The electrolyte leakage was found to be maintained at an almost constant level in JG-62 until 96 h and only showed a marginal increase in later stages of dehydration (Fig. 1*D*). By contrast, ICCV2 showed a sharp rise in electrolyte leakage accompanied by maximal lipid peroxidation (Fig. 1, *C* and *D*). Considering electrolyte leakage and lipid peroxidation, which are considered to be a direct indicator of dehydration tolerance, JG-62 displayed maximum maintenance of cell membrane integrity under dehydration.

Plants that are osmotically adjusted and maintain a high photosynthetic rate have a higher growth rate and higher productivity under dehydration (26). To understand the photosynthetic capabilities of the genotypes studied, the status of photosynthetic pigments, *viz.* chlorophyll *a*, chlorophyll *b*, and carotenoid, was determined in all the varieties under dehydration. Better maintenance of the photosynthetic apparatus was observed in C-235 and JG-62, which also showed the highest protein content under dehydration, whereas maximum damage was observed in Annigiri and ICCV2 (Fig. 2, *A–D*). All the varieties showed an initial decline in photosynthetic pigments, whereas a general increase in pigments was observed around 72 h. It is interesting to note that during this period there was an increase in RWC presumably as a result of increased proline accumulation. It is likely that maintenance of higher RWC in JG-62 because of OA at lowered WP could maintain growth and metabolic activities including photosynthesis and other physiological processes. After 96 h, a constant decline in RWC and proline accumulation indicated the severity of dehydration where OA might fail to maintain the turgor in affected tissues. All together these results suggest JG-62 as a potential dehydration-tolerant variety as compared with the remaining varieties studied.

Dehydration-induced Changes and 2-DE Analysis—Dehydration-induced responses in plants involve nearly every aspect of plant physiology and metabolism. We subjected 3-week-old JG-62 seedlings to gradual dehydration. There were no visible changes in the seedlings during 24 h of dehydration. The leaflets rolled after 36 h of dehydration, and the damage increased further during 48–192 h (Fig. 3). When the dehydrated seedlings were rewatered for 24 h, they fully

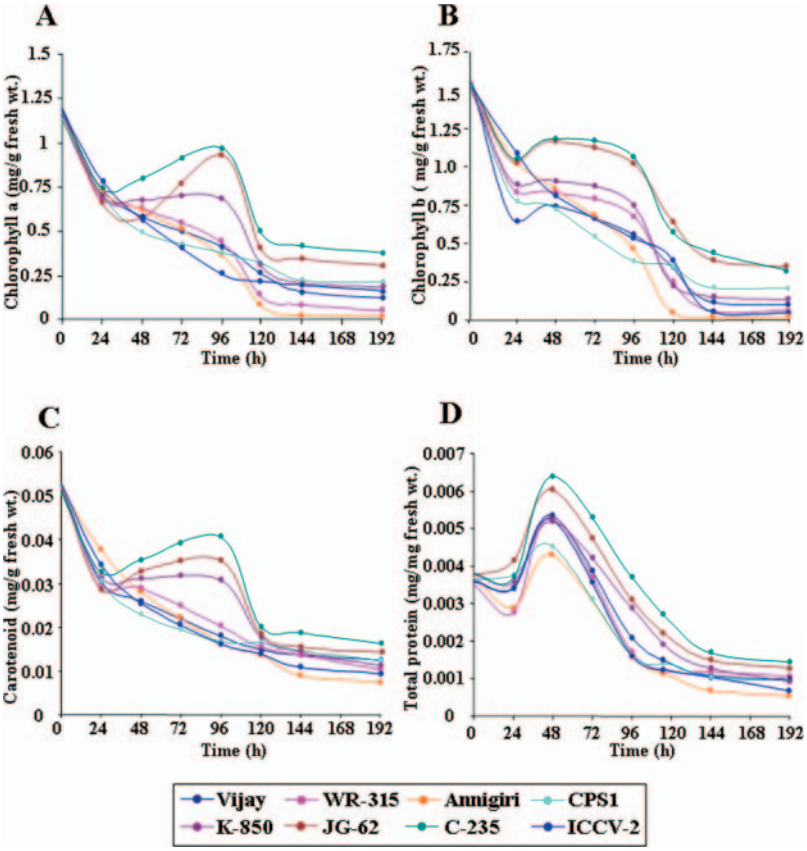

FIG. 2. **Effect of dehydration on photosynthetic pigments and protein content.** Comparative estimation of chlorophyll *a* (*A*), chlorophyll *b* (*B*), carotenoid (*C*), and total protein (*D*) between eight varieties of chickpea in a time-dependent manner under dehydration. All experiments were done in triplicates ($n = 3$), and average mean values were plotted against time.

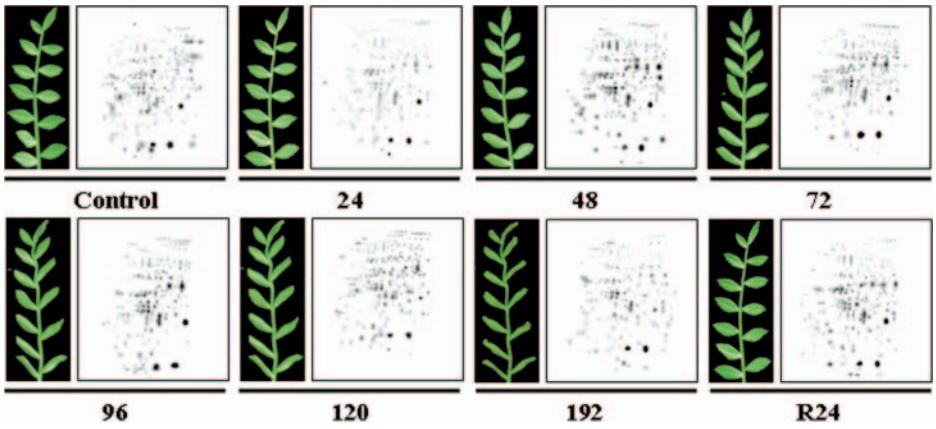

FIG. 3. **Dehydration-induced morphological response in chickpea seedlings and the representative 2-DE gels of ECM proteome.** Three-week-old seedlings were subjected to dehydration and then were allowed to recover for 24 h. The ECM proteins were isolated from the seedlings challenged with dehydration at every 24 h for 192 h duration followed by a recovery stage (*R24*). The photographs of the same sample were taken at each time point, and *framed regions* depict the leaflets from plants under dehydration. An equal amount (125 μg) of protein from each time point was separated by 2-DE. Three replicate gels for each time point were computationally combined using PDQuest software to generate the standard gel.

recovered. The temporal changes in the ECM proteome for the dehydrated as well as stress-recovered seedlings were monitored using 2-DE on proteins isolated from the cell wall-enriched (purified cell wall) fraction during dehydration (0–192 h) followed by a recovery stage as detailed under "Experimental Procedures." The purity of the cell wall fraction was established by transmission electron microscopy and phosphotungstic acid staining (11). The control samples refer to the protein prepared from the pooled unstressed seedlings harvested from different time periods during the course of the experiment to normalize the effect, if any, of growth and development of plants. In addition we compared the ECM

TABLE I
Reproducibility of two-diminensional gels

Time	Average no. of spots[a]	High quality spots[b]	Reproducibility
h			%
Control	271	257	94.83
24	244	228	93.31
48	256	241	94.27
72	278	268	96.28
96	243	220	90.41
120	258	249	96.00
192	287	266	92.57
R24[c]	302	283	93.71
Total	2139	2012	94.06

[a]Average number of spots present in three replicate gels of each time point.
[b] Spots having a quality score more than 30 assigned by PDQuest (version 7.2.0).
[c] Recovery stage.

proteome of unstressed seedlings of day 0 with that of day 8, which showed no significant difference in protein expression (Supplemental Fig. 1). For each time point, three replicate 2-DE gels were run that were then computationally combined into a representative standard gel (first level match set; Supplemental Fig. 2 and Fig. 3). Only those spots that met several stringent criteria (classified as "high quality" spots) were used to estimate spot quantities; otherwise a large number of protein spots were included in the match set. For example, 271 spots were detected in the control gel, but 257 were classified as high quality (Table I). The spot densities at the lower level were normalized against the total density present in the respective gel to overcome the experimental errors introduced due to differential staining. To make comparisons between the time points, a second level match set was created (Fig. 4). A second normalization was done against the densities of unaltered protein spots (Fig. 6, *i–j*). From the higher level match set, the filtered spot quantities were assembled into a data matrix that consisted of 420 unique spots indicating change in intensity for each spot during dehydration. The data reveal that nearly 94% of the spots on the standard gels were of high quality reflecting the reproducibility of the experimental replicates (Table I).

As the set of quantitative proteome data in this study is too large to discuss the relative expression of each individual protein by itself, we analyzed the data by creating statistic and quantitative analysis sets. In the statistic sets, 420 spots were subjected to *t* test at a significance level of 95% resulting in 186 substantially differential spots between the time points. The results revealed 163 DRPs that showed more than 2.5-fold differences in expression values at least at one time point. Of the 163 DRPs, 25 proteins were clearly up-regulated, and 38 proteins were down-regulated, whereas 100 proteins showed a mixed pattern of time-dependent expression. MS/MS analysis was carried out for 134 DRPs resulting in 98 proteins with a significant match, whereas the rest showed no significant match in the database.

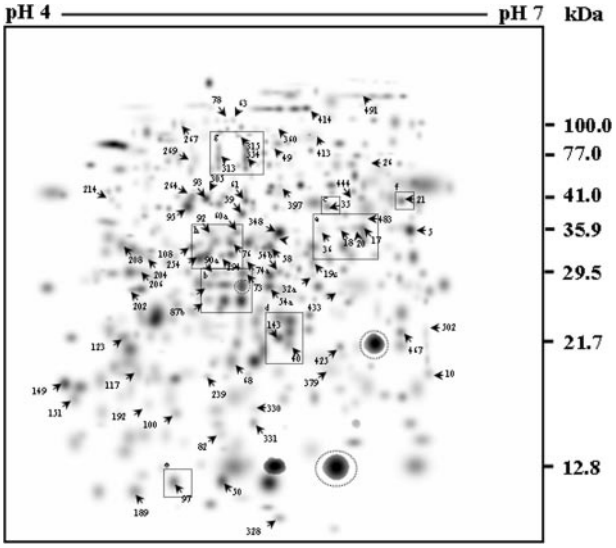

FIG. 4. **Higher level match set of protein spots detected by 2-DE.** The match set was created *in silico* from eight standard gels for each of the time points as depicted in Fig. 3. The *boxed areas* marked with *dotted lines* represent the magnified gel sections, and the *encircled areas* are the representative unaltered spots used for the second normalization. The *numbers* correspond with the spot numbers mentioned in Table II.

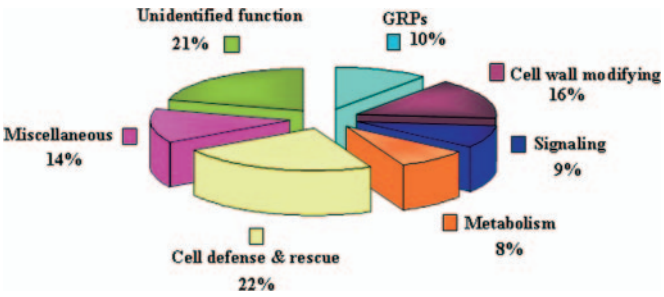

FIG. 5. **Functional cataloging of DRPs in chickpea ECM.** The identified DRPs were assigned a putative function using Pfam and InterPro databases and functionally categorized as represented in the pie chart.

Dehydration-responsive Differential ECM Proteome—Dehydration resistance mechanisms can be classified into two general categories, avoidance and tolerance mechanisms; and accordingly, the dehydration-responsive ECM proteins could be distinguished. The ECM-resident DRPs are expected to play a variety of functions during cellular adaptation against dehydration. A total of 80 DRPs, identified with a significant match, were grouped into six functional classes based on their putative roles in the dehydration response (Fig. 5 and Table II). The protein functions were assigned using a protein function database Pfam (pfam.sanger.ac.uk/) or InterPro (www.ebi.ac.uk/interpro/). The criteria used to address the subcellular localization of the cell wall proteins, in this study, were based on their presence in other reported cell wall proteomes in addition to the predicted biochemical and biological functions.

The communication between the cytoskeleton and the ECM

TABLE II
List of dehydration-responsive chickpea ECM proteins identified by MS/MS analysis

Spot no[a]	Identification	Time Kinetics[b] C 24 48 72 96 120 192 R24	Score	% Coverage	NP[c]	gi No[d]	Thr Mw (kDa)	Exp Mw (kDa)
Glycine Rich Proteins (GRPs)								
CaE-20	Putative glycine-rich RNA-binding protein 2		61	9	1	6911146	16.25	37.2
CaE-117	Putative glycine-rich RNA-binding protein 2		62	15	2	6911146	16.25	19.29
CaE-189	Putative glycine-rich RNA-binding protein 2		61	9	1	6911146	16.25	10.15
CaE-92	Putative glycine-rich RNA-binding protein 2		48	15	2	6911146	16.2	33.5
CaE-63	Putative glycine-rich RNA-binding protein 2		58	22	2	6911142	14.1	60.03
CaE-78	Putative glycine-rich RNA-binding protein 2.-		42	9	1	6911146	16.25	59.88
CaE-354	Putative glycine-rich RNA-binding protein 2		50	9	1	6911146	16.25	50.7
CaE-214	Putative glycine-rich RNA-binding protein 2		50	9	1	6911146	16.25	42.2
Cell wall modifying proteins								
CaE-348	Reversibly glycosylated protein		24	7	1	38194918	38.8	35.5
CaE-305	OSJNBa0042F21.13 protein		143	8	3	38347311	42.21	43.75
CaE-397	se-wap41		221	16	6	1895084	41.17	43.5
CaE-467	Cellulose synthase-like protein		50	2	2	51091927	49.00	23.30
CaE-204	Cellulose synthase-like protein		41	3	2	51091927	49.00	32.5
CaE-60a	Glucan endo-1,3-beta-d-glucosidase precursor		130	8	3	3900936	35.5	36.5

is one of the most characteristic features of cellular mechanics that allows cells to respond effectively to various extracellular signals (27). Several candidate components involved in signal transduction were identified in this study, for example, WAK 4-like protein (CaE-90a), CHRK1 (CaE-483), NDK1 (CaE-10), signal transducer (CaE-458), protein kinase 2 (CaE-399), tubby-like protein (CaE-61), and translation initiation factor (CaE-379). The WAKs relay extracellular signals through their

TABLE II—*continued*

CaE-360	β-N-acetylhexosaminidase-like protein	69	1	1	7019659	63.1	57.3
CaE-26	Methyltetrahydropteroyltriglutamate--homocysteine methyltransferase	96	3	4	974782	84.4	50.0
CaE-140	5-Methyltetrahydropteroyl Methyl transferase	63	3	2	974782	84.5	75.6
CaE-491	Methionine synthase	75	2	2	33325957	87	110.0
CaE-93	Methionine synthase	50	2	2	71000469	84.5	42.5
CaE-267	Methionine synthase	50	1	1	71000469	87.5	58.9
CaE-34	Putative S-adenosyl-L-methionine Mg-protoporphyrin IX methyltransferase	43	2	6	6006382	34.9	40.04
Signaling							
CaE-90a	Wall-associated kinase 4-like	33	3	2	56784949	75.5	30.4
CaE-10	Nucleoside diphosphate kinase I (NDK I)	143	17	2	1346672	16.4	17.10
CaE-61	Tubby-like protein	45	5	2	5689214	47.7	42.0
CaE-483	Receptor-like kinase CHRK1	78	1	1	5814093	83.0	39.9
CaE-399	Protein kinase 2	51	1	1	7573598	45.3	41.7
CaE-379	Translation initiation factor	87	11	2	19601	17.6	20.6
CaE-458	Signal transducer	76	1	1	15229647	59.8	64.04
Metabolism							
CaE-58	Ferredoxin-NADP reductase	45	5	2	2225993	40.0	34.5
CaE-313	NADH dehydrogenase subunit F(Fragment)	44	3	1	45593942	33.5	50.6
CaE-303	Quinone oxidoreductase	161	18	4	21553644	32.7	39.69

TABLE II—*continued*

CaE-5	Ferredoxin:NADP$^+$ reductase, chain A		201	9.7	3	4930123	33.523	35.89
CaE-35	Plastidic aldolase		134	10	4	38096041	43	41.0
CaE-59	Fructose-bisphosphate aldolase precursor		312	17	6	169037	38.6	40.6
Cell defense & Rescue								
CaE-21	Putative mitochondrial NAD-dependent malate dehydrogenase		90	11	3	21388550	36	41.0
CaE-444	Malate dehydrogenase		179	11	3	21388550	36	42.2
CaE-82	Thioredoxin M precursor		45	5	1	4138592	19.1	14.5
CaE-97	Thioredoxin m precursor		102	11	2	481594	19.14	11.0
CaE-76	Chloroplast drought-induced stress protein, putative		53	2	1	21554102	33.7	32.1
CaE-54b	Ascorbate peroxidase		47	1	3	68342454	31	30.7
CaE-73	Ascorbate peroxidase		48	3	1	68342454	31.1	30.47
CaE-206	Chitinase		106	7	2	17942	31.1	30.6
CaE-202	Mannose lectin		69	3	1	6822274	31	28.3
CaE-192	Glyoxalase I		80	6	2	37932483	32.3	16.63
CaE-68	Ferritin 3 precursor	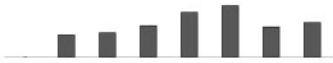	61	3	1	29839257	28	22.0
CaE-87B	Ferritin 3, chloroplast precursor		78	14.6	3	2970652	28	25.46
CaE-40	Ferritin 3, chloroplast precursor		46	14.6	3	29839257	28	22.0
CaE-143	Ferritin	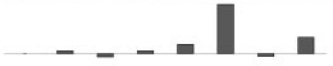	61	3	1	29839257	28.0	22.7
CaE-328	Rps4 (Fragment)		41	6	1	59803301	19	8.9

TABLE II—*continued*

CaE-49	Putative leucine aminopeptidase		54	2	1	47497219	61.7	51.7
CaE-409	aminopeptidase family, catalytic domain	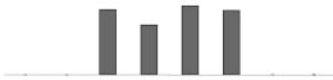	50	2	1	92887207	59.5	54.3
CaE-414	Ferredoxin-dependent glutamate synthase		61	3	1	30721696	30.4	63.2
Miscellaneous								
CaE-151	ATP synthase beta subunit (Fragment)		53	7	2	7708306	49.05	20.0
CaE-123	ATP synthase beta subunit (Fragment)		41	5	2	3850902	52.69	23.0
CaE-315	Mitochondrial chaperonin-60		48	3	2	22758324	60.8	55.5
CaE-294	Aspartate carbamoyltransferase	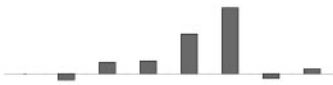	44	2..3	1	15796550	42.74	32.4
CaE-16	Aspartate carbamoyl transferase		44	2	1	15796550	42.0	28.9
CaE-208	Mannitol transporter		47	3	2	85070363	56	34.6
CaE-95	Sedoheptulose bisphosphatase		125	6	3	22136118	42.4	42.48
CaE-425	Aspartate carbamoyl transferase		46	2	1	15796550	42.5	21.7
CaE-18	Epoxide hydrolase		38	2	1	20975616	30.8	37.27
CaE-19c	Protein T23G18.2		42	1	2	6579214	301.63	30.6
CaE-215	Peptidyl-prolyl cis-trans isomerase		62	2	4	10720315	49.8	44.33
Unidentified function								
CaE-330	Hypothetical protein		42	2	3	15222664	55.45	16.4
CaE-50	Hypothetical protein		51	2	3	53370738	104.1	11.02
CaE-149	Hypothetical protein OJ1641_C04.130		38	3	1	50934411	24.73	18.36

TABLE II—*continued*

CaE-54a	Hypothetical protein P0413C03.2		49	1	8	34906958	28.3	28.73
CaE-81	Os08g0412500		47	1	7	115476396	12.06	15.2
CaE-99	Unknown protein		47	2	6	22655728	38.7	43.42
CaE-106	Os07g0123800		58	3	14	115470403	16.6	24.54
CaE-119	unknown protein		41	1	4	15238284	22.7	20.3
CaE-32b	Unknown protein		48	1	4	77416969	25.6	30.06
CaE-56	hypothetical protein		48	1	3	86438763	26.5	25.9
CaE-255	hypothetical protein		48	1	3	86438763	26.5	33.7
CaE-438	hypothetical protein		46	3	1	56784832	36.1	30.95
CaE-59b	unnamed protein product		46	1	2	116057698	41.4	39.32
CaE-362	Hypothetical protein At1g55040		41	1	2	1529314	94.7	54.53
CaE-74a	Hypothetical protein OSJNBa0051D19.2		61	5	1	10140719	25.8	32.3
CaE-234	Hypothetical protein T5M16.19		43	1	2	12323390	147.11	14.4
CaE-470	OSJNBb0039F02.4	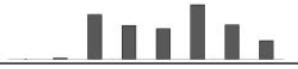	57	2	7	21742316	26.9	33.07

[a] Spot number as given on the 2-D gel images. The first letters (Ca) signify the source plant, *C, arietinum*, followed by the subcellular fraction, ECM (E). The numerals indicate the spot numbers corresponding to Fig. 4.

[b] Time kinetics represents the average change in spot density at various time points C (control) and 24, 48, 72, 96, 120, 192, and R24 (recovery stage) h. The data were taken in terms of -fold expression with respect to the control value and were log-transformed to the base 2 to level the scale of expression and to reduce th noise.

[c] NP represents the number of peptides.

[d] Gene identification number as in GenBank™.

cytoplasmic kinase domain. They are known to bind glycine-rich proteins (GRPs; CaE-20, -63, -78, -92, -117, -189, -214, and -354) and to a 2C-type protein phosphatase in the cytoplasm and form a signalosome complex (28). These results suggest that WAKs might play a critical role in dehydration tolerance. CHRK1 belongs to the family of receptor kinases where it has a chitinase (CaE-206)-specific interacting domain. Both CHRK1 and chitinase were found to be up-regulated between 48 and 120 h of dehydration. These proteins are known to be induced under different environmental stresses (29), and elucidating their possible role in dehydration tolerance is of importance. NDK1 is known to interact with cytosolic catalases and play a role in relieving oxidative stress (30). It is also an important component for maintaining stable GTP levels through nucleotide homeostasis in various GTP-mediated signal transduction pathways (31). The tubby-like protein (CaE-61) was found to be up-regulated at 72 h. It belongs to the F-box family proteins that encode transcription factors and is known in animals to shuttle between the plasma membrane and the nucleus on environmental cue (32). Unusual proteins like translation initiation factor were also observed that may play a more diverse role in ECM than in its classical com-

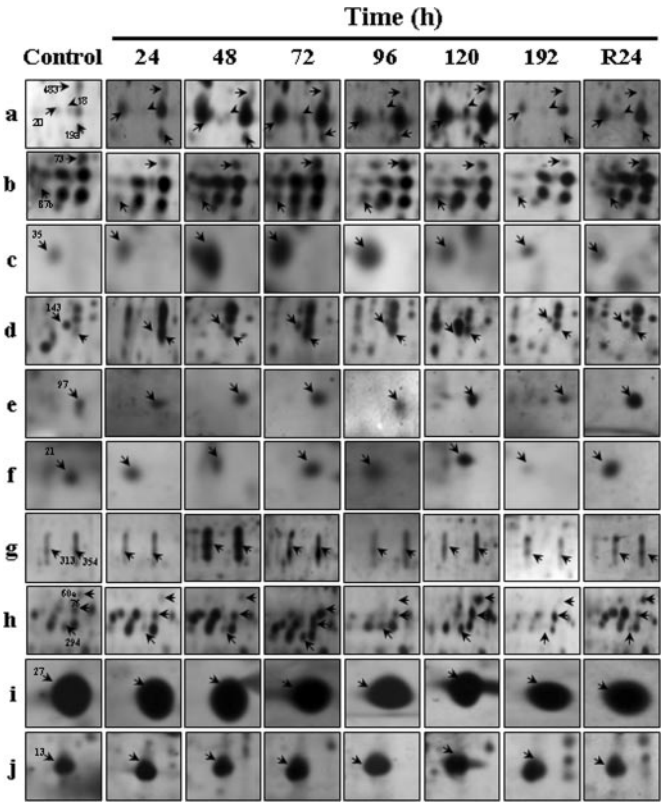

FIG. 6. **Time-dependent changes of the differentially expressed proteins.** *Boxed areas* (*a–h*) are magnified gel sections and correspond to the *framed regions* (*a–h*) in Fig. 4. The unaltered protein spots are represented in *i* and *j*.

partment. The differential regulation of different components of the signaling network in ECM suggests that there is a complicated mechanism controlling the perception and transduction of various extracellular signals during dehydration.

As mentioned above, the JG-62 seedlings showed a drop in cellular RWC after 24 h followed by an increased accumulation of proline in the next 48 h (Fig. 1, *A* and *B*). It is suggested that the mechanism of dehydration avoidance involves accumulation of compatible solutes and cell wall modification. A cellulose synthase (CaE-204 and -467) was detected at 24 and 48 h but could not be detected during 72–120 h of dehydration. This could be due to an increase in the accumulation of certain soluble sugars probably through inhibiting enzymes involved in cellulose biosynthesis (33). For example, glycosyl hydrolases such as β-galactosidase (CaE-60a; Fig. 6*h*), xyloglucan hydrolase (CaE-305), and hexosaminidase (CaE-360) utilize cell wall polysaccharides as an alternate carbon source under sugar depletion in the cytoplasm. Furthermore sedoheptulose (CaE-95) earlier identified in the secondary cell walls of pea was implicated to serve as an alternative sugar in the developing xylem (34). It is assumed that under stress ECM serves as an alternative source for sugar moieties that are redirected in the cytosol for turgor maintenance. An alternate mechanism to avoid water loss under dehydration could be the lignification of the cell wall, and a step toward this is the methylation of the lignin monomers. The methylation of the lignin precursors is carried out by *S*-adenosylmethionine synthetase from *S*-adenosylmethionine, a common methyl group donor. The expression of genes encoding methionine synthase (CaE-26, -93, -140, -267, and -491) contributes to the production of methionine from which *S*-adenosylmethionine is generated (35, 36). This might be explained by a demand for more methyl groups for lignin methylation.

A sharp drop in both RWC and proline accumulation was observed in JG-62 seedlings (Fig. 1, *A* and *B*) after 96 h of dehydration, indicating their inability to maintain the turgor in affected tissues. It is conceivable that with a further drop of RWC it becomes increasingly difficult to avoid dehydration, and thus mechanisms to tolerate water deficit become important. Peroxides and other redox compounds play an important role in the stress perception of the apoplast, which acts as a bridge between the environment and the symplast (37). The direct measure of peroxides in the cell comes from estimating lipid peroxidation under dehydration. Under progressive dehydration, lipid peroxidation increased drastically after 96 h with a concurrent drop in RWC (Fig. 1), indicating the severity of the stress condition.

Reactive oxygen species (ROS) produced under dehydration can act as signaling molecules for the stress response, but above a certain threshold they can cause damage to many cellular components. Most of the dehydration tolerance mechanisms primarily involve protection of the cellular structure wherein an important method is the control of the level of ROS or the limitation of damage caused by ROS. It is reported that NADH is generated by the malate dehydrogenase (CaE-21 and -444; Fig. 6*f*) and used to form H_2O_2 (38) possibly by NADH oxidase on the plasmalemma. Alternately quinone oxidoreductase (CaE-303) produces peroxides by oxidizing quinones, which are generated by diamine oxidases (39). Plants control ROS levels through sophisticated mechanisms such as scavenging them by peroxidases like ascorbate peroxidase (CaE-54b and -73; Fig. 6*b*). In addition thioredoxin (CaE-76, -82, and -97; Fig. 6, *e* and *h*) is also involved in redox regulation by reducing disulfides on the target protein and relaying the signal to MAPKK (mitogen-activated protein kinase kinase) pathway of stress signaling (40). Earlier we identified a chickpea ECM ferritin (11), which is known to sequester the highly reactive Fe^{3+} and prevent the formation of toxic $OH^{\bullet}$ species (41). We showed, for the first time, that the ECM ferritin (CaE-87b, -68, -40, and -143) is induced by dehydration (Fig. 6, *b* and *d*) and might play a crucial role in dehydration tolerance. Other redox proteins such as ferredoxin-NADP reductase and NADH dehydrogenase are also involved in the ROS pathway (42, 43). Another interesting protein that was expressed only under stress conditions was mannose lectin (CaE-202). There are reports suggesting that cell wall lectins may be involved in compensatory mechanisms, which stabi-

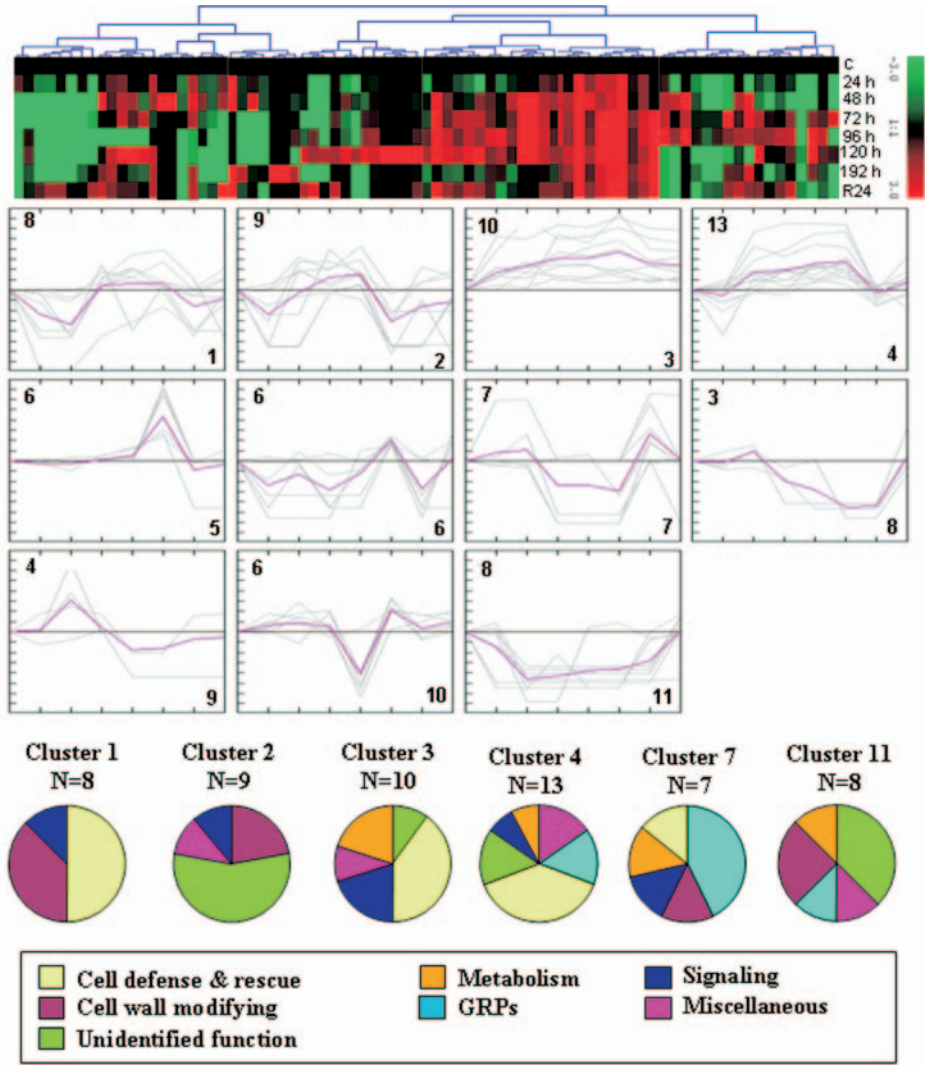

FIG. 7. **Clustering analysis of expression profiles of DRPs in chickpea.** The 80 differentially expressed proteins were clustered into 11 clusters based on their expression profiles. The SOTA cluster tree is shown at the *top*, and the expression profiles in SOTA clusters are shown *below*. The expression profile of each individual protein in the cluster is depicted by *gray lines* while the mean expression profile is marked in *pink* for each cluster. The number of proteins in each cluster is given in the *left upper corner*, and the cluster number is given in the *right lower corner*. Detailed information on proteins within each cluster can be found in Supplemental Fig. 3.

lize the cytoskeleton structure under stress conditions (44). Furthermore aldolases (CaE-35 and -59) are known to act as adhesion molecules between ECM and the cytoskeleton and may be involved in cross-talk between the extracellular space and the cell interior (45).

The involvement of multiple dehydration-responsive components in a variety of cellular functions is important in understanding and solving the problems of such stress tolerance. There are several reports that suggest extensive cross-talk among environmental stress-responsive pathways (7, 46, 47). We observed the expression of chitinase (CaE-206), between 48 and 120 h of dehydration, that is known to be induced under osmotic stress (1). The Rps 4 fragment (CaE-328), an R gene, was detected exclusively at 192 h of dehydration. The GRPs form a novel class of proteins that play pleiotropic roles both in osmotic stress and biotic stress (48). Induction of GRPs at different time intervals of dehydration could be attributed to their multiple roles (Fig. 6*a*). The role of glyoxalase-1 (CaE-192) under salt stress has been well studied (49). Although glyoxalase-1 has been detected in cell wall proteomes of maize and *Medicago* (50, 51), its role in the ECM and its involvement in dehydration response are not understood. Proteins like leucine aminopeptidase (CaE-49) and glutamate synthase (CaE-414) are known to be induced under various abiotic and biotic stresses and modulate the turnover of selected peptide or protein populations under stress (52, 53). Glutamate synthase particularly regulates the accumulation of proline in osmotically stressed plants (54). Candidates like epoxide hydrolase (CaE-18) are induced under fungal stress, although its role under dehydration is not known. Roles of miscellaneous dehydration-responsive candidates like aspartate carbamoyltransferase (CaE-294) and ATP synthase (CaE-123, 151) need to be evaluated.

In this study, several differentially expressed proteins appeared to be the products of degradation because their observed M_r values were much smaller than the theoretical

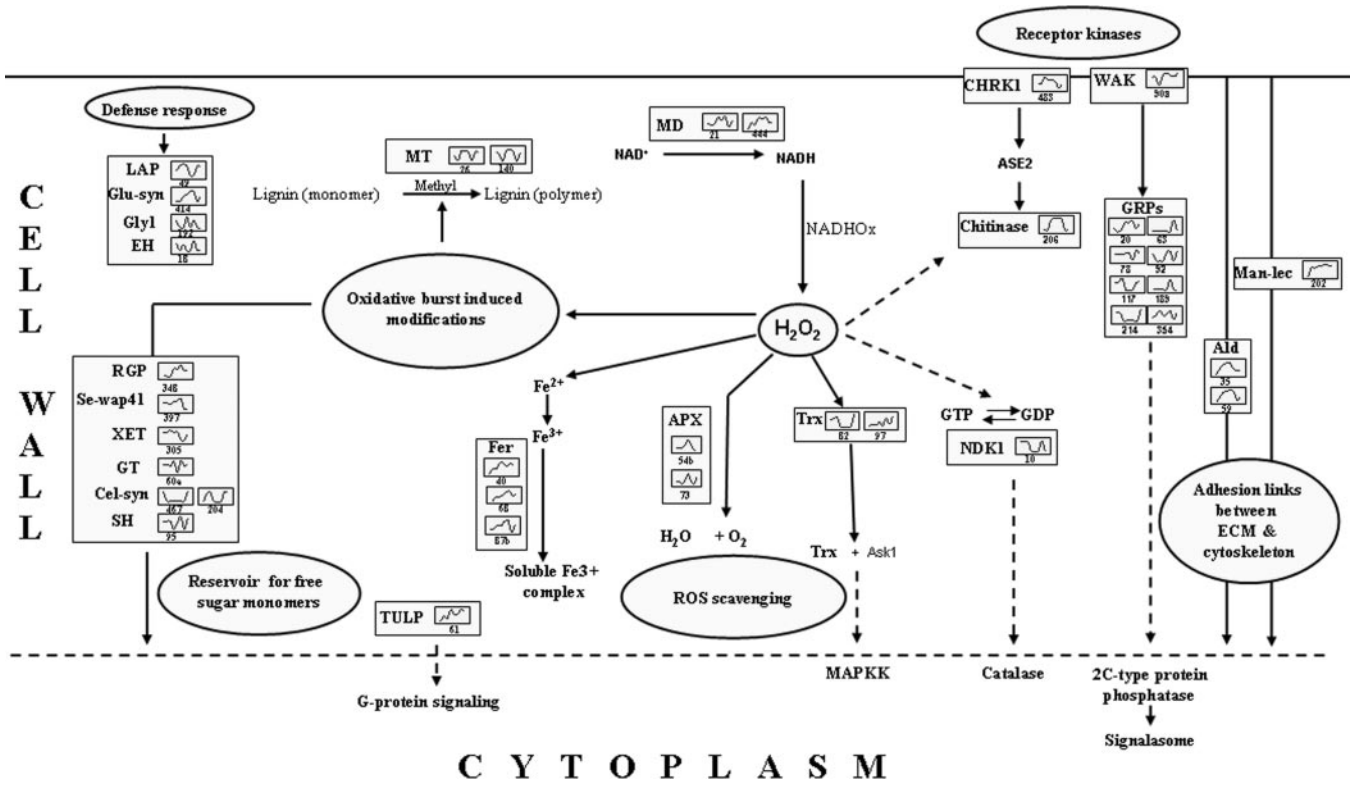

FIG. 8. **Pathways involved in cell defense, signaling, and cell wall modification under dehydration stress in chickpea ECM.** Proteins identified in this study are indicated in the *box* and are displayed on the corresponding metabolic pathways. *Graphs* are representatives of the expression profile of an individual protein, and the *number* given *below* each graph indicates the protein identification number. *APX*, ascorbate peroxidase; *MD*, malate dehydrogenase; *LAP*, leucine aminopeptidase; *Glu-syn*, glutamate synthase; *Gly1*, glyoxalase-1; *EH*, epoxide hydrolase; *RGP*, reversibly glycosylated peptides; *XET*, xyloglugan endotransglycosylase; *Cel-syn*, cellulose synthase; *SH*, sedoheptulose, *GT*, glycosyltransferase; *TULP*, tubby-like protein; *Fer*, ferritin; *Trx*, thioredoxin; *MT*, methyltransferase; *Ald*, aldolase; *Man-lec*, mannose lectin; *MAPKK*, mitogen-activated protein kinase kinase; *NADHOx*, NADH oxidase.

values. We observed this phenomenon in a few class of proteins including cell wall-modifying enzymes (cellulose synthase and methionine synthase), signaling proteins (wall-associated kinase 4 and receptor kinase CHRK1), and cell defense and rescue (glyoxalase-1) among others. A particular case was that of methionine synthase represented by three spots (Table II). The observed M_r values of two of the spots (CaE-93 and -267) were smaller than the theoretical M_r values, which might be due to the stress-responsive degradation of proteins (55–57). As previously noted, this stress-responsive degradation of proteins can be attributed to the ROS-mediated pathway (58). It is very likely that ROS may also account for the degradation of other proteins.

Expression Profile of Dehydration-responsive Proteins—To achieve a comprehensive overview of expression profile in terms of protein function, SOTA clustering was done for the 80 DRPs. The data were taken in terms of -fold expression with respect to the control expression value. In addition the data sets were log-transformed to the base 2 to level the scale of expression and to reduce the noise. The analysis yielded 11 expression clusters, and only the clusters with $n > 6$ were used to study the co-expression patterns for functionally similar proteins (Fig. 7). Detailed information on proteins within each cluster can be found in Supplemental Fig. 3.

The most abundant group, Clusters 3 and 4, were found to be early dehydration-responsive and showed induction at all time points reaching maxima at 96–120 h. These groups were found to be enriched in proteins involved in cell defense and rescue. The time span of expression of cell defense proteins entails the kinetics of dehydration tolerance in chickpea, JG-62 in particular. Proteins involved in signaling, cell wall modification, and metabolism displayed a diverse and complex pattern of regulation (Clusters 1, 2, 4, and 11) wherein no clear clustering pattern was observed. The cellular defense strategy seems to be dependent on the advancement of dehydration, and thus both early and late responses could be seen. Also the miscellaneous class of proteins showed no clear clustering patterns, which may be due to heterogeneous composition of this class. However, co-expression patterns were observed for proteins with unidentified function (Clusters 2 and 11), and identification of these proteins can provide valuable insight into kinetics of dehydration tolerance mechanisms.

Conclusions—In plants, the mechanisms of dehydration avoidance *versus* tolerance form the basis for understanding

and interpreting the dehydration-responsive events, which may help in formulating strategies for defense. Nevertheless there are many overlapping mechanisms that fragment the line between these two events of dehydration adaptation. For example, accumulation of compatible solutes such as proline plays an important role in dehydration avoidance by maintenance of RWC. Alternately accumulation of proline has been proposed to play a role in dehydration tolerance by protecting protein and membrane structure, regulating redox status, or acting as a scavenger of ROS (59–61). It should also not be assumed that dehydration avoidance and/or tolerance occurs in a linear progression in time after dehydration sets in. In the study of plant responses to dehydration, the important consideration would be the method used to impose the dehydration, the severity and duration of the dehydration, the physiological status to be assessed, and how the observed responses of the plant fit into an overall strategy for adaptation to dehydration. Although major attention has been focused on plant responses to dehydration at the cellular level, an integrated approach comprising physiological and molecular biology techniques that may improve the basic understanding of complex genotypes *versus* dehydration is rare. This study was aimed at understanding cell physiology under dehydration and its effects in terms of changes in organelle-specific protein expressions in chickpea. The results obtained have been illustrated as a representative model to summarize the events modulating dehydration tolerance (Fig. 8). The perception of dehydration condition is presumably regulated by water status of the plant. The fall in RWC in the first 24 h of dehydration seemingly resulted in induction of signaling proteins. Probable osmotic adjustment was seen as a result of compatible solute accumulation in the next 48 h. Plants undergo cell wall modifications to minimize water loss and avoid dehydration condition. Cell defense pathway-related proteins are induced in later stages that perhaps aid the survival of plants under severe dehydration. Also probable linkers between the cytoskeleton and ECM may relay biochemical/mechanical signals induced by dehydration to the interior of the cell. These findings would bridge the gap between the events of ecophysiological experiments and comparative proteomics analysis in elucidating the molecular mechanisms by which plants sense and respond to dehydration stress. Comparative proteomics analysis is a promising tool for determination of components involved in dehydration tolerance, although the number of proteins that can be analyzed by 2-DE is still limited with respect to the predicted number of proteins. A considerable number of candidates (21%) were found to be unknown or hypothetical proteins. As many as 36 DRPs showed no significant match in the existing database. The results are particularly important, at least in part, due to the fact that the genome sequence of chickpea has not been determined yet, and the number of fully annotated expressed sequence tags is very low. Our future efforts will focus on identifying the dynamics associated with the ECM-resident proteins involved in the dehydration response and determining their functions, which would provide the basis for effective engineering strategies for a crop improvement program.

* This work was supported by grants from the Department of Biotechnology, Ministry of Science and Technology (to N. C.) and by predoctoral fellowships (to D. B., A. P., and M. K. C.) from the Council of Scientific and Industrial Research, Government of India. The costs of publication of this article were defrayed in part by the payment of page charges. This article must therefore be hereby marked "*advertisement*" in accordance with 18 U.S.C. Section 1734 solely to indicate this fact.

S The on-line version of this article (available at http://www.mcponline.org) contains supplemental material.

‡ To whom correspondence may be addressed. Tel.: 91-11-26735186; Fax: 91-11-26716658; E-mail: subhrac@hotmail.com.

§ To whom correspondence may be addressed. Tel.: 91-11-26735178; Fax: 91-11-26716658; E-mail: nchakraborty@hotmail.com.

REFERENCES

1. Bray, E. A. (2004) Genes commonly regulated by water-deficit stress in Arabidopsis thaliana. *J. Exp. Bot.* **55,** 2331–2341
2. Chaves, M. M., and Oliveira, M. M. (2004) Mechanisms underlying plant resilience to water deficits: prospects for water-saving agriculture. *J. Exp. Bot.* **55,** 2365–2384
3. Chaves, M. M., Maroco, J. P., and Pereira, J. S. (2003) Understanding plant response to drought: from genes to the whole plant. *Funct. Plant Biol.* **30,** 239–264
4. Flexas, J., Bota, J., Cifre, J., Escalona, J. M., Galmés, J., Gulías, J., Lefi, E.-K., Florinda, S. Cañellas, M., Moreno, M. T., Ribas-Carbó, M., Riera, D., Sampol, B., and Medrano, H. (2004) Understanding downregulation of photosynthesis under water stress: future prospects and searching for physiological tools for irrigation management. *Ann. Appl. Biol.* **144,** 273–283
5. Blum, A. (2005) Drought resistance, water-use efficiency, and yield potential—are they compatible, dissonant, or mutually exclusive? *Aust. J. Agri. Res.* **56,** 1159–1168
6. Clark, A. J., Landolt, W., Bucher, J. B., and Strasser, R. J. (2000) Beech (*Fagus sylvatica*) response to ozone exposure assessed with a chlorophyll *a* fluorescence performance index. *Environ. Pollut.* **109,** 501–507
7. Seki, M., Narusaka, M., Ishida, J., Nanjo, T., Fujita, M., Oono, Y., Kamiya, A., Nakajima, M., Enju, A., Sakurai, T., Satou, M., Akiyama, K., Taji, T., Yamaguchi-Shinozaki, K., Carninci, P., Kawai, J., Hayashizaki, Y., and Shinozaki, K. (2002) Monitoring the expression profiles of 7000 Arabidopsis genes under drought, cold and high-salinity stresses using a full-length cDNA microarray. *Plant J.* **31,** 279–292
8. Shinozaki, K., and Yamaguchi-Shinozaki, K. (1997) Gene expression and signal transduction in water-stress response. *Plant Physiol.* **115,** 327–334
9. Westbrook, J. A., Wheeler, J. X., Wait, R., Welson, S. Y., and Dunn, M. J. (2006) The human heat proteome: two-dimensional maps using narrow range immobilised pH gradients. *Electrophoresis* **27,** 1547–1555
10. Dreger, M. (2003) Proteome analysis at the level of subcellular structures. *Eur. J. Biochem.* **270,** 589–603
11. Bhushan, D., Pandey, A., Chattopadhyay, A., Choudhary, M. K., Chakraborty, S., Datta, A., and Chakraborty, N. (2006) Extracellular matrix proteome of chickpea (*Cicer arietinum* L.) illustrates pathway abundance, novel protein functions and evolutionary perspect. *J. Proteome Res.* **5,** 1711–1720
12. Pandey, A., Choudhary, M. K., Bhushan, D., Chattopadhyay, A., Chakraborty, S., Datta, A., and Chakraborty, N. (2006) The nuclear proteome of chickpea (*Cicer arietinum* L.) reveals predicted and unexpected proteins. *J. Proteome Res.* **5,** 3301–3311
13. Clarke, S. E. (2001) Cell signaling at the shoot meristem. *Nat. Rev. Mol. Cell. Biol.* **2,** 276–284
14. Shibaoka, H., and Nagai, R. (1994) The plant cytoskeleton. *Curr. Opin. Cell Biol.* **6,** 10–15
15. Jamet, E., Canut, H., Boudart, G., and Pont-Lezica, R. F. (2006) Cell wall

proteins: a new insight through proteomics. *Trends Plant Sci.* **11,** 33–39
16. Carpita, N. C., and Gibeaut, D. M. (1993) Structural models of primary cell walls in flowering plants: consistency of molecular structure with the physical properties of the walls during growth. *Plant J.* **3,** 1–30
17. Barker, D. G., Bianchi, S., Blondon, F., Dattee, Y., Duc, G., Essad, S., Flament, P., Gallusci, P., Genier, G., Guy, G., Muel, X., Tourneur, J., Denarie, J., and Huguet, T. (1990) *Medicago truncatula*, a model plant for studying the molecular genetics of the *Rhizobium*-legume symbiosis. *Plant Mol. Biol. Rep.* **8,** 40–49
18. Singh, K. B., Ocampo, B., and Robertson, L. D. (1998) Diversity for abiotic and biotic stress resistance in the wild annual *Cicer* species. *Genet. Res. Crop Evol.* **45,** 9–17
19. Winter, P., Benko-Iseppon, A. M., Huttel, B., Ratnaparkhe, M., Tullu, A., Sonnante, G., Pfaff, T., Tekeoglu, M., Santra, D., Sant, V. J., Rajesh, P. N., Kahl, G., and Muehlbauer, F. J. (2000) A linkage map of the chickpea (*Cicer arietinum* L.) genome based on recombinant inbred lines from a *C. arietinum* x *C. reticulatum* cross: localisation of resistance genes for Fusarium wilt races 4 and 5. *Theor. Appl. Genet.* **101,** 1155–1163
20. Silva, M., Purcell, L. C., and King, C. A. (1996) Soybean petiole ureide response to water deficits and decreased transpiration. *Crop Sci.* **36,** 611–616
21. Bates, L. S., Waldren, R. P., and Teare, I. D. (1973) Rapid determination of free proline for water stress studies. *Plant Soil* **39,** 205–207
22. Chakarborty, N., and Tripathy, B. C. (1992) Involvement of singlet oxygen in 5-aminolevulinic acid induced photodynamic damage of cucumber (*Cucumis sativus* L.) chloroplasts. *Plant Physiol.* **98,** 7–11
23. Casey, T. M., Arthur, P. G., and Bogoyevitch, M. A. (2005) Proteomic analysis reveals different protein changes during endothelin-1- or leukemic inhibitory factor-induced hypertrophy of cardiomyocytes in vitro. *Mol. Cell. Proteomics* **4,** 651–661
24. Romijin, E. P., Christis, C., Wieffer, M., Gouw, W. J., Fullaondo, A., Sluijs, P., Braakman, I., and Heck, A. J. R. (2005) Expression clustering reveals detailed co-expression patterns of functionally related proteins during B cell differentiation. *Mol. Cell. Proteomics* **4,** 1297–1310
25. Blum, A. (1996) Developing drought and low N-tolerant maize, in *Proceedings of a Symposium at the International Maize and Wheat Improvement Center (CIMMYT), El-Batan, March 25–29 1996* (Edmeades, G. O., Banziger, M., Mickelson, H. R., and Pena-Valdivia, C. B., eds) pp. 131–135, CIMMYT, El-Batan, Mexico
26. Moinuddin, A., and Chopra, R. K. (2004) Crop physiology and metabolism. *Crop Sci.* **44,** 449–455
27. Baluska, F., Samaj, J., Wojtaszek, P., Volkmann, D., and Menzel, D. (2003) Cytoskeleton-plasma membrane-cell wall continuum in plants. Emerging links revisited. *Plant Physiol.* **133,** 482–491
28. Anderson, C. M., Wagner, T. A., Perret, M., He, Z. H., He, D., and Kohorn, B. D. (2001) WAKs: cell wall-associated kinases linking the cytoplasm to the extracellular matrix. *Plant Mol. Biol.* **47,** 197–206
29. Hong, J. K., and Hwang, B. K. (2002) Induction by pathogen, salt and drought of basic class II chitinase mRNA and its in situ localization in pepper (*Capsicum annum*). *Physiol. Plant* **114,** 549–558
30. Fukamatsu, Y., Yabe, N., and Hasunuma, K. (2003) Arabidopsis NDK1 is a component of ROS signaling by interacting with three catalases. *Plant Cell Physiol.* **44,** 982–998
31. Pan, A., Kawai, M., Yano, A., and Uchimiya, H. (2000) Nucleoside diphosphate kinase required for coleoptile elongation in rice. *Plant Physiol.* **122,** 447–452
32. Lai, C. P., Lee, C. L., Chen, P. H., Wu, S. H., Yang, C. C., and Shaw, J. F. (2004) Molecular analyses of the Arabidopsis TUBBY-like protein gene family. *Plant Physiol.* **134,** 1586–1597
33. Chen, Z., Hong, X., Zhang, H., Wang, Y., Li, X., Zhu, J. K., and Gong, Z. (2005) Disruption of the cellulose synthase gene, AtCesA8/IRX1, enhances drought and osmotic stress tolerance in *Arabidopsis. Plant J.* **43,** 273–283
34. Anderson, L. E., and Andrew, A. C. (2004) Seven enzymes of carbon metabolism, including three Calvin cycle isozymes, are present in the secondary cell wall thickenings of the developing xylem tracheary elements in pea leaves. *Int. J. Plant Sci.* **165,** 243–256
35. Ravanel, S., Gakiere, B., Job, D., and Douce, R. (1998) The specific features of methionine biosynthesis and metabolism in plants. *Proc. Natl. Acad. Sci. U. S. A.* **23,** 7805–7812
36. Ravanel, S., Block, M. A., Rippert, P., Jabrin, S., Curien, G., Rebeille, F., and Douce, R. (2004) Methionine metabolism in plants: chloroplasts are autonomous for de novo methionine synthesis and can import S-adenosylmethionine from the cytosol. *J. Biol. Chem.* **279,** 22548–22557
37. Yan, S. P., Zhang, Q. E., Tang, Z. C., Su, W. A., and Sun, W. N. (2006) Comparative proteomic analysis provides new insights into chilling stress response in rice. *Mol. Cell. Proteomics* **5,** 484–496
38. Gross, G. G., Janse, C., and Elstner, E. F. (1977) Involvement of malate, monophenols and superoxide radical in hydrogen peroxide formation by isolated cell walls from horseradish (*Armoracia lapathifolia Gilib*). *Planta* **136,** 271–276
39. Vianello, A., and Macri, F. (1991) Generation of superoxide anion and hydrogen peroxide at surface of plant cells. *J. Bioenerg. Biomembr.* **23,** 409–423
40. Apel, K., and Hirt, H. (2004) Reactive oxygen species: metabolism, oxidative stress and signal transduction. *Annu. Rev. Plant Biol.* **55,** 373–399
41. Mittler, R., Vanderauwera, S., Gollery, M., and van Breusegem, F. (2004) The reactive oxygen gene network of plants. *Trends Plant Sci.* **9,** 490–498
42. Taylor, A. R., and Chow, R. H. (2001) A microelectrochemical technique to measure trans-plasma membrane electron transport in plant tissue and cells in vivo. *Plant Cell Environ.* **24,** 1–6
43. Kenneth, A., Jensen, J. R., Houtman, C. J., Zachary, C. R., and Kenneth, E. H. (2001) Pathways for extracellular Fenton chemistry in the brown rot basidiomycete *Gloeophyllum trabeum. Appl. Environ. Microbiol.* **67,** 2705–2711
44. Garaeva, L. D., Pozdeeva, S. A., Timofeeva, O. A., and Khokhlova, L. P. (2006) Cell-wall lectins during winter wheat cold hardening. *Russ. J. Plant Physiol.* **53,** 746–750
45. Jewett, T. J., and Sibley, L. D. (2003) Aldolase forms a bridge between cell surface adhesins and the actin cytoskeleton in apicomplexan parasites. *Mol. Cell* **11,** 885–894
46. Yamaguchi-Shinozaki, K., and Shinozaki, K. (1994) A novel cis-acting element in an Arabidopsis gene is involved in responsiveness to drought, low-temperature, or high-salt stress. *Plant Cell* **6,** 251–264
47. Cheong, Y. H., Chang, H. S., Gupta, R., Wang, X., Zhu, T., and Luan, S. (2002) Transcriptional profiling reveals novel interactions between wounding, pathogen, abiotic stress and hormonal responses in *Arabidopsis. Plant Physiol.* **129,** 661–677
48. Mousavi, A., and Hotta, Y. (2005) Glycine-rich proteins: a class of novel proteins. *Appl. Biochem. Biotechnol.* **120,** 169–174
49. Singla-Pareek, S. L., Reddy, M. K., and Sopory, S. K. (2003) Genetic engineering of the glyoxalase pathway in tobacco leads to enhanced salinity tolerance. *Proc. Natl. Acad. Sci. U. S. A.* **100,** 14672–14677
50. Zhu, J., Chen, S., Alvarez, S., Asirvatham, V. S., Schachtman, D. P., Wu, Y., and Sharp, R. E. (2006) Cell wall proteome in maize primary root elongation zone. I. Extraction and identification of water soluble and lightly ionically bound proteins. *Plant Physiol.* **140,** 311–325
51. Watson, B. S., Lei, Z., Dixon, R. A., and Sumner, L. W. (2004) Proteomics of *Medicago sativa* cell walls. *Phytochemistry* **65,** 1709–1720
52. Gu, Y. Q., Chao, W. Y., and Walling, L. L. (1996) Localization and post-translational processing of the wound-induced leucine aminopeptidase proteins of tomato. *J. Biol. Chem.* **271,** 25880–25887
53. Hirose, N., and Yamaya, T. (1999) Okadaic acid mimics nitrogen-stimulated transcription of the NADH-glutamate synthase gene in rice cell cultures. *Plant Physiol.* **121,** 805–812
54. Díaz, P., Borsani, O., Márquez, A., and Monza, J. (2005) Osmotically induced proline accumulation in *Lotus corniculatus* leaves is affected by light and nitrogen source. *Plant Growth Regul.* **46,** 223–232
55. Hajduch, M., Rakwal, R., Agrawal, G. K., Yonekura, M., and Pretova, A. (2001) High-resolution two-dimensional electrophoresis separation of proteins from metal-stressed rice (*Oryza sativa* L.) leaves: drastic reductions/fragmentation of ribulose-1,5-bisphosphate carboxylase/oxygenase and induction of stress-related proteins. *Electrophoresis* **22,** 2824–2831
56. Agarwal, G. K., Rakwal, R., Yonekura, M., Kubo, A., and Saji, H. (2002) Proteome analysis of differentially displayed proteins as a tool for investigating ozone stress in rice (*Oryza sativa* L.) seedlings. *Proteomics* **2,** 947–959
57. Zhao, C. F., Wang, J. Q., Cao, M. L., Zhao, K., Shao, J. M., Lei, T. T., Yin,

J. N., Hill, G. G., Xu, N. Z., and Liu, S. Q. (2005) Proteomic changes in rice leaves during development of field-grown rice plants. *Proteomics* **5,** 961–972
58. Desimone, M., Henke, A., and Wagner, E. (1996) Oxidative stress induces partial degradation of the large subunit of ribulose-1,5-bisphosphate carboxylase/oxygenase in isolated chloroplasts of barley. *Plant Physiol.* **111,** 789–796
59. Hare, P. D., Cress, W. A., and van Staden, J. (1998) Dissecting the roles of osmolyte accumulation during stress. *Plant Cell Environ.* **21,** 535–553
60. Hincha, D. K., and Hagemann, M. (2004) Stabilization of model membranes during drying by compatible solutes involved in the stress tolerance of plants and microorganisms. *Biochem. J.* **383,** 277–283
61. Verslues, P. E., and Sharp, R. E. (1999) Proline accumulation in maize (*Zea mays* L.) primary roots at low water potentials. II. Metabolic source of increased proline deposition in the elongation zone. *Plant Physiol.* **119,** 1349–1360